Removal of Cationic Tolonium Chloride Dye Using Fe_3O_4 Nanoparticles Modified with Sodium Dodecyl Sulfate

M. H. Abedi,[a] M. Ahmadmoazzam,[b,c] and N. Jaafarzadeh[b,d,*]

[a]Department of Chemical Engineering, Mahshahr Branch, Islamic Azad University, Mahshahr, Iran

[b]Department of Environmental Health Engineering, Ahvaz Jundishapur University of Medical Sciences, Ahvaz, Iran

[c]Student Research Committee, Ahvaz Jundishapur University of Medical Sciences, Ahvaz, IR Iran

[d]Environmental Technologies Research Center, Ahvaz Jundishapur University of Medical Sciences, Ahvaz, Iran

doi: 10.15255/CABEQ.2017.1245

Original scientific paper
Received: October 25, 2017
Accepted: May 28, 2018

In this study, Fe_3O_4 nanoparticles modified with sodium dodecyl sulfate (Fe_3O_4-SDS) were used for the adsorption of cationic tolonium chloride (TC) dye from aqueous solution. The effects of temperature, pH, amount of nanoparticles and SDS concentration, stirring time, and interfering ions on dye adsorption were investigated. For TC, the maximum removal was 98 % in the best conditions (pH = 6; 0.6 g Fe_3O_4-SDS; 30 °C temperature, and 3 min stirring time). Data from the sorption kinetic studies showed the best fitting of the pseudo-second-order model for adsorption of the dye. The Langmuir isotherm showed better fitting of the data for TC adsorption by Fe_3O_4-SDS compared with the other models. The Fe_3O_4-SDS nanoparticles are easily synthesizable, magnetically recoverable, and regenerable, which increases their practical applications. Additionally, NaCl showed no significant impact on the dye removal up to 0.8 molar concentration, which increases the industrial application of the process.

Keywords:
magnetite nanoparticles, tolonium chloride, sodium dodecyl sulfate, adsorption

Introduction

Dye removal is one of the most important parameters in wastewater treatment.[1] Dyes must be removed not only because of their appearance, but also dyes can combine with chlorine and form halogenated compounds that are harmful and carcinogenic.[2,3] Many industries, including textile, dyeing, paper making, cosmetics, pharmaceuticals, etc., use these compounds extensively.[4] Discharge of waste containing these compounds into the environment is harmful to human health and damages the ecosystem, because they are usually non-biodegradable and toxic.[5] Therefore, appropriate techniques for treating these types of wastewater are required. Due to their low biodegradability features, biological treatment methods are not usually able to effectively remove the dye compounds from the wastewater.[6] Different methods, including various physicochemical methods, such as coagulation-flocculation,[7] ultra and nanofiltration,[8,9] reverse osmosis,[10] electrocoagulation,[11–13] advanced oxidation processes,[14–16] chemical oxidation,[17] and adsorption on different materials[18] have been studied by many researchers. Most of the proposed methods for the removal of dyes have low efficiency, according to the time required for removal. Adsorption methods by nanomaterials are excellent techniques for dye removal from wastewater due to their efficiency, high surface area, high reactivity properties, and catalytic potential, in addition to the simplicity of design.[19,20] Adsorption by metal nanoparticles is an environmentally friendly technology, which has been considered in recent years as a suitable method to remove organic contaminants and heavy metal ions from water and wastewater.[21] In recent years, the use of Fe_3O_4 magnetic nanoparticles (Fe_3O_4 NPs) has been considered in water and wastewater treatment due to its many advantages.[22,23] In addition to high adsorption ability, magnetic nanoparticles have the advantage of easy separation by a strong magnetic field, which is important in terms of their recycling and reuse.[24] By applying a magnetic field to a magnetic fluid, the magnetic particles stick together and form a solid. The main problem with this method is that the fine particles dispersed in the liquid tend to agglomerate and form larger particles, and therefore reduce their magnetic

*Corresponding author: Neemat Jaafarzadeh;
E-mail: Jaafarzadeh-n@ajums.ac.ir; Phone number: +98-09163184501

features.[25] In order to overcome this problem and increase their application, the Fe_3O_4 surface is usually modified with different agents.[26,27] Modification of the surface of nanoparticles with agents, such as polymers or surface-active compounds (surfactants), can prevent their agglomeration. Surfactants attach to the nanoparticles and create a repulsive force between them thus preventing agglomeration. The modification of Fe_3O_4 NPs with surfactants, such as sodium dodecyl sulfate (SDS), has been reported as an appropriate and facile way to improve Fe_3O_4 performance.[28–30] The Fe_3O_4 NPs modified with SDS have been reported in 2011 for removal of safranin O dye from aqueous solutions.[30] Faraji *et al.* reported the SDS-coated Fe_3O_4 NPs as a solid-phase extraction adsorbent for the extraction of Hg(II) from water samples.[29] Furthermore, high-efficiency extraction of fluoxetine using the Fe_3O_4 NPs modified with SDS from aquatic and urine samples have been reported in 2011.[28]

In this study, we aimed to modify the Fe_3O_4 NPs surface with sodium dodecyl sulfate as a facile modification way to improve the adsorption efficiency of the magnetic nanoparticles, which exhibit a high efficiency for tolonium chloride removal from aqueous solutions. The effect of different parameters, such as pH, dye concentration, temperature, and ions intervention on process performance was investigated. The experimental data were also analyzed to study the adsorption kinetics and isotherms.

Material and methods

Materials

Iron oxide nanopowder (Fe_3O_4), with diameter of 20–30 nm and purity of 99.5 % was purchased from US Research Nanomaterials, Inc. (USA). TEM image of the purchased Fe_3O_4 is shown in Fig. 1. Sodium dodecyl sulfate (SDS), as an anionic surfactant ($NaC_{12}H_{25}SO_4$), was purchased from Merck (Germany). The tolonium chloride, $C_{15}H_{16}ClN_3S$ (molar mass: 270.374 g mol^{-1}) as a cationic dye with more than 99 % purity, was provided by Sigma-Aldrich (USA). Fig. 2 shows the molecular structure of tolonium chloride and sodium dodecyl sulfate. Other materials, high-purity methanol (>99 %), phosphoric acid (84–85 %), and hydrochloric acid (37 %) were provided from Merck (Germany).

Analytical methods

The concentration of the tolonium chloride dye was measured using a UV-Vis spectrophotometer (Varian Cary 100, USA) with quartz cells, measuring the absorbance at λ_{max} = 632 nm. The pH was measured with a portable pH-meter (Mettler Toledo-Seven Easy, Switzerland). A magnet with strength of 1.5 Tesla was used to separate the nanoparticles from solution.

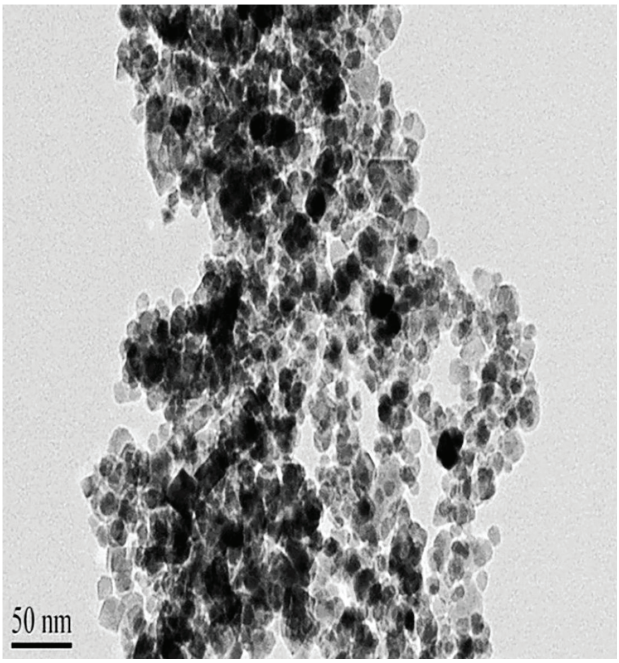

Fig. 1 – *TEM image of the purchased Fe_3O_4*

Preparation of magnetic Fe_3O_4-SDS

Sodium dodecyl sulfate 0.5 % solution (%w/v) was prepared by adding 0.5 g of sodium dodecyl sulfate salt to a 100-mL volumetric balloon, and dissolved in distilled water. In order to cover the iron oxide nanoparticles with the SDS, one mL of 0.5 % SDS solution was added to a beaker containing 0.6 grams of iron oxide nanoparticles, and stirred with a glass rod for two minutes.[28,30] The resulting magnetic Fe_3O_4-SDS was then separated from the solution with a magnet, and washed several times with deionized water to remove the residual surfactant.

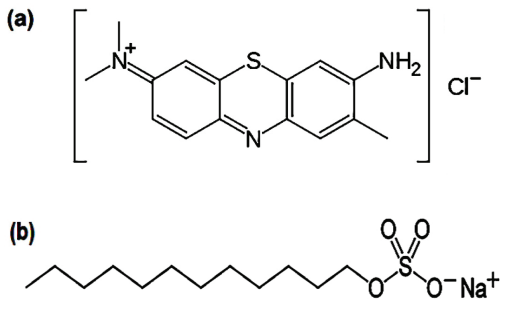

Fig. 2 – *Molecular structure of tolonium chloride (a) and sodium dodecyl sulfate (b)*

Batch adsorption experiments

The adsorption experiments of tolonium chloride on Fe_3O_4-SDS were performed through a batch process. The dye solution, containing 20 mg L^{-1}, was prepared by dissolving 0.02 g tolonium chloride in 1000 mL deionized water. The solution of 0.1 M phosphoric acid and 0.1 M NaOH were used for the preparation of phosphate buffer solution with pH = 6, and used to adjust the initial pH of the solution. Firstly, 10 mL of 20 mg L^{-1} tolonium chloride solution and 3 mL of buffer solution were added to a 100-mL volumetric balloon and filled with distilled water. The concentration of the dye in prepared and control solutions was measured with a UV-Vis spectrophotometer at λ_{max} = 632 nm. Thereafter, 0.6 g of Fe_3O_4-SDS was added to an Erlenmeyer flask containing 100 mL of the prepared dye solution and stirred for two minutes. After stirring, the flask was placed in the magnetic field for adsorbent separation. The adsorption capacities (mg g^{-1}) and removal efficiency (%) were finally calculated by equations (1) and (2), respectively:

$$q_e = \frac{(C_o - C_e)\cdot V}{m} \quad (1)$$

$$\text{Removal efficiency} = \frac{C_o - C_t}{C_o}\cdot 100 \quad (2)$$

where q_e (mg g^{-1}) is the amount of dye adsorbed on the adsorbent (adsorption capacities), C_o and C_t are concentrations of the dye (mg L^{-1}) at the initial time and at time t, respectively, V (mL) is the volume of dye solution, C_e is the equilibrium concentration of dyes (mg L^{-1}), and m (g) is the weight of Fe_3O_4-SDS.

Results and discussion

Effect of pH variation

The effect of pH variation on the adsorption of TC onto Fe_3O_4-SDS was evaluated in a pH range of 3–12. This pH range was selected because when Fe_3O_4 NPs are dissolved at a pH less than 3, it causes darkening of the solution.[28] Also, at a pH higher than 12, the magnetic nanoparticles shift to colloidal particles and do not respond to magnetic fields. As shown in Fig. 3, the adsorption of the dye increased with pH increasing from 3 to 6, and then decreased as the pH increased from 6 to 12. The maximum TC removal of 98.1 % was obtained at pH 6. According to the zeta potential, the Fe_3O_4 particles have isoelectric point at pH 6.5.[31] Therefore, the positively charged surface of Fe_3O_4 NPs in the solution created suitable conditions for higher adsorption of anionic surfactants; hence, the cationic

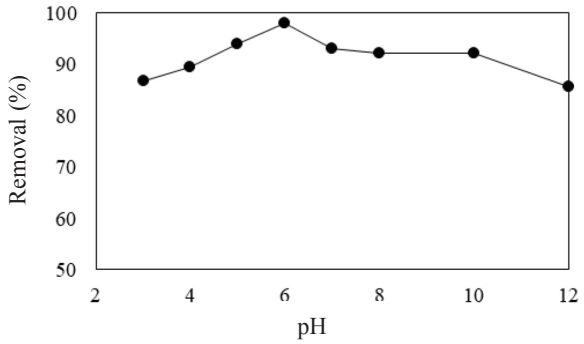

Fig. 3 – *Effect of pH variation on removal efficiency of TC onto Fe_3O_4-SDS. Test conditions: 100 mL TC solution (2 mg L^{-1}); 0.6 g of Fe_3O_4 covered with one mL of 0.5 % SDS solution and 2 min stirring time (100 rpm).*

dye removal increased.[28] Also, removal reduction at lower pH (< 6) can be due to the competition of H^+ ions with the cationic dye, which prevented the complete adsorption of the dye cations onto the negative clouds surrounding the nanoparticles due to repulsive force.[32] In addition, at alkali pH, more available hydroxyl ions in solution will encompass the cationic dye molecules and decrease the positively charged at the dye surface. Therefore, the electrostatic attraction decreased between the ionic adsorbent head groups ($–SO_3–$) and cationic dye molecules surrounded by hydroxyl ions.[30,33]

Effect of magnetic nanoparticles doses and SDS concentration

The effect of adsorbent doses on the adsorption efficiency of the dye was studied with the addition of 0.25 and 0.65 g of the Fe_3O_4 NPs to 100 mL of the dye solution. As shown in Fig. 4a, with the use of more nanoparticles, because of the presence of more adsorption sites, the dye removal efficiency also increased from 66.3 to 98.2 % for nanoparticles mass of 0.25 and 0.6 g, respectively, and then it was almost fixed. Therefore, 0.6 g of the Fe_3O_4 NPs was used as an optimum amount for the next experiments.

In addition, the effect of the SDS concentration for modification of the surface of Fe_3O_4 NPs was investigated in a concentration range of 0.1 to 0.62 % (w/v). The surfactant can help the adsorption of the cationic dye on the surface of the Fe_3O_4 by increasing the negative charge on the adsorbent surface.[25,29] According to the obtained results, dye molecules were efficiently removed with a higher amount of SDS added to the solution, and the dye removal increased to 98.7 % with the maximum amount of 0.62 % (w/v) (Fig. 4b). This phenomenon was due to the fact that the repulsion force had decreased between the cationic dye and positive surface charge of the Fe_3O_4 NPs when more adsorbent was coated with the SDS.[30] As the removal ef-

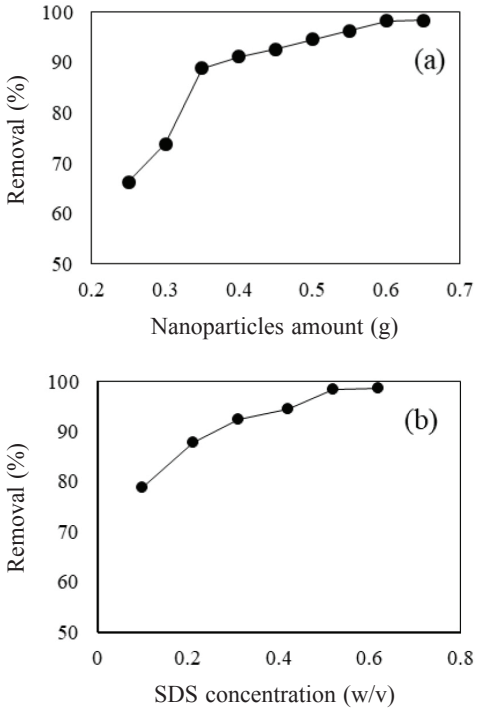

Fig. 4 – *Effect of magnetic nanoparticles amount and SDS concentration on removal efficiency of TC onto Fe_3O_4-SDS. Test conditions: pH = 6; 100 mL TC solution (2 mg L^{-1}), and 2 min stirring time (100 rpm).*

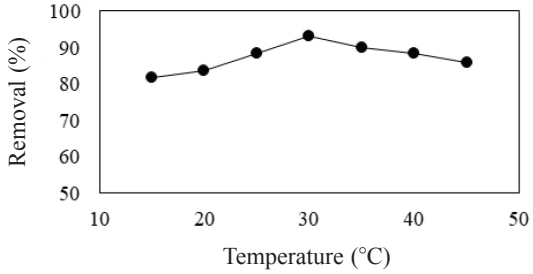

Fig. 5 – *Effect of temperature on removal efficiency of TC onto Fe_3O_4-SDS. Test conditions: pH = 6; 100 mL TC solution (2 mg L^{-1}); 0.6 g Fe_3O_4-SDS, and 2 min stirring time (100 rpm).*

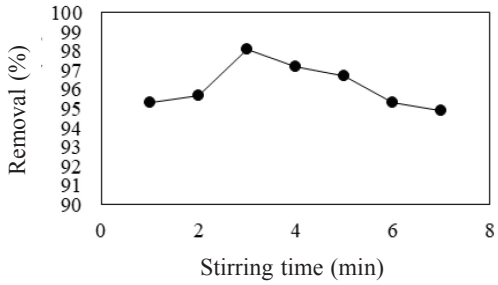

Fig. 6 – *Effect of temperature on removal efficiency of TC onto Fe_3O_4-SDS. Test conditions: pH = 6; 100 mL TC solution (2 mg L^{-1}); 0.6 g Fe_3O_4-SDS, and 30 °C temperature.*

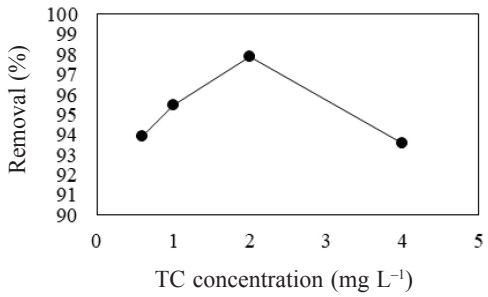

Fig. 7 – *Effect of initial concentration on removal efficiency of TC onto Fe_3O_4-SDS. Test conditions: pH = 6; 0.6 g Fe_3O_4-SDS; 30 °C temperature, and 3 min stirring time (100 rpm).*

ficiency was constant with the SDS addition, more than 0.52 % (w/v), this value was selected for the next experiments.

Temperature effect

According to the literature, temperature is a main factor in the adsorption process.[5,32] Therefore, the temperature effect on TC adsorption efficiency onto Fe_3O_4-SDS was studied in the temperature range of 15–45 °C at 100 mL TC solution (2 mg L^{-1}), and 0.6 g Fe_3O_4-SDS (Fig. 5). Removal of TC dye revealed that the process was relatively dependent on temperature. The data trend showed that the dye removal increased with temperature from 15 to 30 °C, and then a reduction in removal efficiency was observed at the temperature above 30 °C, which verified that TC dye adsorption was an exothermic process. The highest removal efficiency was 93.3 % at a temperature of 30 °C. At lower temperature, a lower kinetic energy of the dye molecules could cause an insufficient collision between TC and adsorbent surface, and decrease the removal efficiency.[34] Also, lower adsorption at temperatures above 30 °C might be due to the higher kinetic energy of the TC molecules than the adsorption potential between TC molecules and adsorbent surface, which weakens the absorbing force.[35,36] In addition, the desorption process of the adsorbed molecules may start with temperature rising.[32]

Effect of stirring times and TC dye initial concentration

Experiments were carried out at different stirring times (1 to 7 min) to study the contact time effect on the removal efficiency of TC dye onto Fe_3O_4-SDS. As shown in Fig. 6, at the beginning of the experiment, adsorption efficiency rapidly increased with time and showed the maximum removal of 98.1 % after 3 min reaction, and then slightly decreased. This was because, at the beginning of the experiment, all the adsorbent sites were empty, and therefore, the dye molecule adsorption on the adsorbent surface increased with increasing time. Over time, with the saturation of adsorption sites, adsorption reduced and eventually reached adsorption and desorption equilibrium.[6,37]

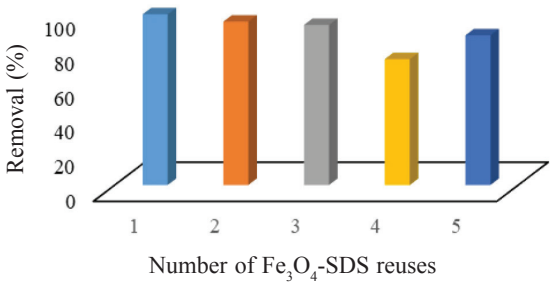

Fig. 8 – *Removal efficiency of TC during five repeated usages of Fe_3O_4-SDS. Test conditions: pH = 6; 100 mL TC solution (2 mg L^{-1}); 0.6 g Fe_3O_4-SDS; 30 °C temperature, and 3 min stirring time (100 rpm).*

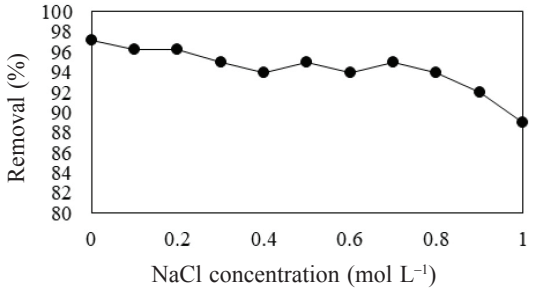

Fig. 9 – *Effect of NaCl concentration on removal efficiency of TC onto Fe_3O_4-SDS. Test conditions: pH = 6; 100 mL TC solution (2 mg L^{-1}), and 3 min stirring time (100 rpm).*

The effect of initial dye concentration on the removal efficiency of TC dye at different concentrations (0.6 to 4 mg L^{-1} with fixed 0.6 g of Fe_3O_4-SDS) is indicated in Fig. 7. The results showed that the removal percentage increased as the concentration increased from 0.6 to 2 mg L^{-1}, and then decreased with higher concentration. This phenomenon can easily be explained in terms of the fact that each adsorbent has a specific adsorption site that is saturated with increasing concentrations above a certain level. Studies from other researchers showed similar results.[34,38,39]

Adsorbent reusability study

Fig. 8 shows the ability of Fe_3O_4-SDS of adsorbing a certain amount of TC during 5 consecutive cycles. The removal rate eventually decreased to 92.5 % after repeating the process three times, and by repeating the process for the fourth cycle the removal efficiency decreased finally to 72 %. At the last cycle, the adsorption was measured after washing the adsorbent with methanol. The result showed that the removal rate increased to 86.5 % after desorption step with methanol.

Effect of NaCl concentration and ions intervention

The effect of NaCl concentration (as an electrolyte) on the removal efficiency of the TC onto Fe_3O_4-SDS was studied (Fig. 9). In addition, to investigate the effect of ionic strength, varying amounts of Cl^-, CO_3^{2-}, Mg^{2+}, Ca^{2+}, and K^+ were added to the solution. Interfering effects of three dyes (Rose Bengal, Amaranth, and Thionine) on the removal efficiency of the TC was also studied. The dye removal rate of 150 mL dye solution (2 mg L^{-1}) was 98.6 %, and this amount was considered as a reference for comparison with other results. If other result variations are less than ±5 % of the reference amount, the results are acceptable and the expected ion concentration is not disturbing. Table 1 shows the maximum concentration for every case in which

Table 1 – *Effect of ions and dyes intervention on TC removal*

Type of studied ions and dyes	Maximum concentration without interference (mg L^{-1})
Cl^-, CO_3^{2-}, Mg^{2+}, Ca^{2+}, K^+	1000
Rose Bengal and Amaranth	200
Thionine	100
Fe^{3+}	50
Fe^{2+}	25

Table 2 – *Fe_3O_4-SDS performance for TC removal from petrochemical effluent*

Petrochemical industries (No.)	TC concentration (mg L^{-1})	Removal (%)
1	3	99.4
	5	97.1
2	3	99.3
	5	99.4
3	3	99.6
	5	97.2

the TC removal varied less than ±5 % of the reference amount. The results showed that the interfering agents have little effect on the TC removal process even at high concentrations. Finally, to evaluate the effectiveness of Fe_3O_4-SDS nanoparticles in real terms, three petrochemical effluents were used as the reaction matrix and the removal efficiency was measured under the previously mentioned optimal conditions. As previous tests have shown, the disturbing ions in wastewater have little impact on process performance (Table 2).

Kinetics and adsorption isotherms

In adsorption experiments, a kinetic analysis is very important to understand the details and mechanisms of the adsorption functions.[40] The adsorption

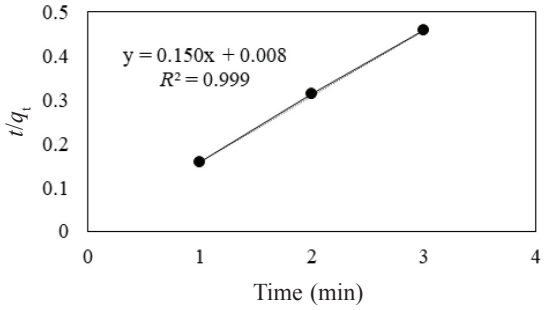

Fig. 10 – *Plotting the pseudo-second-order kinetic model in optimum conditions*

kinetic analysis predicts the adsorption rate in addition to the capacity of adsorbents for the removal of contaminants, which are important for designing and modeling these processes. The contact time required for complete adsorption is achieved using adsorption rate. Analyzing the kinetic data for adsorption of the TC onto Fe_3O_4-SDS was determined using the pseudo-first-order and pseudo-second-order models for expression of the adsorption rate.[41] The kinetic studies were done in a 250-mL glass beaker filled with 100 mL TC solution (2 mg L^{-1}) added to 0.6 g Fe_3O_4-SDS at 30 °C, and 100 rpm stirring speed. The kinetic model rate constants were calculated using the line equations obtained from the kinetic models plotting and pseudo-first-order and pseudo-second-order model equations (equation 3 and 4, respectively) as follows:

$$\log(q - q_t) = \log(q_e) - \frac{k_1 t}{2.303} \tag{3}$$

$$\frac{t}{q_t} = \frac{}{k_2 q} + \frac{t}{q_e} \tag{4}$$

where q_e and q_t are adsorption capacity at equilibrium and time t in mg g^{-1}, and k_1 and k_2 are pseudo-first-order and pseudo-second-order rate constants in min^{-1} and g mg^{-1} min^{-1}, respectively. Fig. 10 shows the fitting of kinetic data to the pseudo-second-order kinetic model. The obtained value for the rate constant (k_2) and adsorption capacity at equilibrium (q_e) for pseudo-second-order model were 2.81 g mg^{-1} min^{-1} and 6.66 mg g^{-1}, respectively. Also, k_1 and q_e were calculated as 0.152 min^{-1} and 0.21 mg g^{-1}, respectively, for pseudo-first-order model. The higher value of the rate constant (k_2) and equilibrium adsorption capacity (q_e) for pseudo-second-order model showed the best fitting of the pseudo-second-order model for adsorption of the TC onto Fe_3O_4-SDS, and confirmed the higher adsorption potential in pseudo-second-order model due to the chemisorption mechanism via electrostatic attraction.[30]

In this study, the equilibrium isotherm equations of Langmuir, Freundlich, and Temkin were used to describe the adsorption behavior and predict the adsorption pattern in a batch study. 150 mL of the TC solution in the concentration range of 2–20 mg L^{-1} was added to a glass jar containing 0.6 g of adsorbent. The amount of the TC adsorbed onto the Fe_3O_4-SDS was obtained after reaching the equilibrium time. In order to select the most appropriate isotherm equations, they were drawn in linear form and isotherm constants were then obtained. Linear forms of the adsorption isotherm models are as follows:

– Langmuir equation[42]

$$\frac{C_e}{q_e} = \frac{1}{q_{max} \cdot b} + \frac{1}{q_{max}} C_e \tag{5}$$

where q_e (mg g^{-1}) is the equilibrium concentration of the adsorbed dye onto the adsorbent, C_e (mg L^{-1}) the equilibrium concentration of the dye in solution, q_{max} (mg g^{-1}) the maximum monolayer capacity of the adsorbent, b (L mg^{-1}) the Langmuir constant and related to the strength of the adsorption energy. In the Langmuir isotherm model, the q_{max} and b values can be obtained by linear regression of $\frac{C_e}{q_e}$ versus C_e in which $\frac{1}{q_{max}}$ and $\frac{1}{q_{max} \cdot b}$ are slope and intercept of plotted linear graph, respectively (Fig. 11a).

– Freundlich equation[43]

$$\log q_e = \log(k_f) + \frac{1}{n} + \log C_e \tag{6}$$

where k_f (L g^{-1}) and n (dimensionless) are the Freundlich constant and show the adsorption capacity of the adsorbent and the heterogeneity factor, respectively. Then n and k_f values can be calculated respectively from the slope and intercept of the line by drawing $\log q_e$ versus $\log C_e$ (Fig. 11b).

– Temkin equation[44]

$$q_e = A + B \cdot \log C_e \tag{7}$$

where A (adsorption potential in the initial state (mg g^{-1})), and B (stability of adsorption (L mg^{-1})) are the Temkin isotherm constants, and are respectively the intercept and slope of the plotted linear regression of q_e versus $\log C_e$ (Fig. 11c).

Fig. 11 shows the calculated coefficients for the adsorption isotherms of the TC onto the Fe_3O_4-SDS. Comparison of the obtained values for constants and regression coefficients in accordance with these three models offered the Langmuir model (R^2 = 0.9975) as better fitting of the data for TC adsorption by the Fe_3O_4-SDS compared with the Freun-

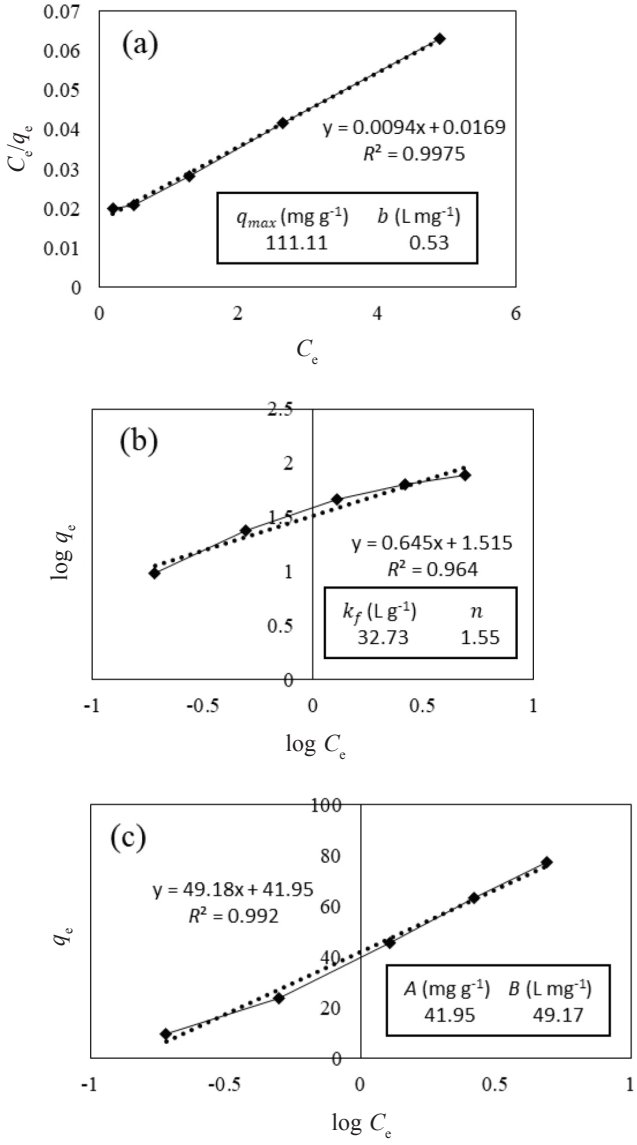

Fig. 11 – *Graph plotted for calculating q_{max} and b in the Langmuir model (a), k_f and n in Freundlich model (b), and A and B constants in Temkin model (c)*

dlich (R^2 = 0.9645) and Temkin (R^2 = 0.9922) models. The Langmuir constant values were calculated as 111.11 mg g^{-1} and 0.53 L mg^{-1}, respectively. The higher values for the Langmuir constant (b) showed that more surface of adsorbent was covered by adsorbed molecules due to the stronger tendency of the molecules to the surface.[45,46] The q_{max} value is the maximum capacity of the adsorbent and its high value confirmed an appropriate adsorption capacity for TC adsorption by the Fe_3O_4-SDS.[4]

Conclusions

Iron oxide nanoparticles modified with sodium dodecyl sulfate surfactant (Fe_3O_4-SDS) were successfully utilized as an efficient adsorbent to remove the tolonium chloride dye from wastewater samples. Maximum removal of the dye was achieved at 98 % in optimum conditions (pH = 6; 0.6 g Fe_3O_4-SDS; 30 °C temperature, and 3 min stirring time). In this study, the cations interference was very low and no significant impact of real wastewater cations was observed on removal efficiency. Additionally, NaCl (as an electrolyte), showed no significant impact on the dye removal up to 0.8 molar concentration, which increases the industrial application of the process. The kinetic study showed the best fitting of the pseudo-second-order model for adsorption of the TC onto Fe_3O_4-SDS and confirmed chemisorption mechanism. The Langmuir model showed better fitting of the data for TC adsorption by the Fe_3O_4-SDS compared with the Freundlich and Temkin models. In addition, Fe_3O_4-SDS nanoparticles are easily synthesizable, magnetically recoverable and regenerable, which increases their practical applications.

ACKNOWLEDGMENT

The present paper was prepared from MSc thesis in Chemical Engineering: Environmental Engineering. This research received no specific grant from funding agencies in the public, commercial, or non-profit sectors.

References

1. *Azari, A., Gholami, M., Torkshavand, Z., Yari, A., Ahmadi, E., Kakavandi, B.*, Evaluation of basic Violet 16 adsorption from aqueous solution by magnetic zero valent iron-activated carbon nanocomposite using Response Surface Method: Isotherm and kinetic studies, J. Mazandaran Uni. Med. Scin. **24** (2015) 333. doi: https://doi.org/10.1016/j.jcis.2017.02.025
2. *Lei, C., Pi, M., Kuang, P., Guo, Y., Zhang, F.*, Organic dye removal from aqueous solutions by hierarchical calcined Ni-Fe layered double hydroxide: Isotherm, kinetic and mechanism studies, J. Colloid Interface Sci. **496** (2017) 158. doi: https://doi.org/10.1016/j.jcis.2017.02.025
3. *Jaafarzadeh, N., Ghanbari, F., Moradi, M.*, Photo-electro-oxidation assisted peroxymonosulfate for decolorization of acid brown 14 from aqueous solution, Korean J. Chem. Eng. **32** (2015) 458. doi: https://doi.org/10.1007/s11814-014-0263-4
4. *Konicki, W., Aleksandrzak, M., Moszyński, D., Mijowska, E.*, Adsorption of anionic azo-dyes from aqueous solutions onto graphene oxide: Equilibrium, kinetic and thermodynamic studies, J. Colloid Interface Sci. **496** (2017) 188. doi: https://doi.org/10.1016/j.jcis.2017.02.031
5. *Konicki, W., Hełminiak, A., Arabczyk, W., Mijowska, E.*, Removal of anionic dyes using magnetic Fe@graphite core-shell nanocomposite as an adsorbent from aqueous solutions, J. Colloid Interface Sci. **497** (2017) 155. doi: https://doi.org/10.1016/j.jcis.2017.03.008

6. *Garg, V., Gupta, R., Yadav, A.B., Kumar, R.*, Dye removal from aqueous solution by adsorption on treated sawdust, Bioresour. Technol. **89** (2003) 121. doi: https://doi.org/10.1016/S0960-8524(03)00058-0
7. *Riera-Torres, M., Gutiérrez-Bouzán, C., Crespi, M.*, Combination of coagulation–flocculation and nanofiltration techniques for dye removal and water reuse in textile effluents, Desalination. **252** (2010) 53. doi: https://doi.org/10.1016/j.desal.2009.11.002
8. *Alventosa-deLara, E., Barredo-Damas, S., Alcaina-Miranda, M., Iborra-Clar, M.*, Ultrafiltration technology with a ceramic membrane for reactive dye removal: Optimization of membrane performance, J. Hazard. Mater. **209** (2012) 492. doi: https://doi.org/10.1016/j.jhazmat.2012.01.065
9. *Hedayatipour, M., Jaafarzadeh, N., Ahmadmoazzam, M.*, Removal optimization of heavy metals from effluent of sludge dewatering process in oil and gas well drilling by nanofiltration, J. Environ. Manage. **203** (2017) 151. doi: https://doi.org/10.1016/j.jenvman.2017.07.070
10. *Nataraj, S., Hosamani, K., Aminabhavi, T.*, Nanofiltration and reverse osmosis thin film composite membrane module for the removal of dye and salts from the simulated mixtures, Desalination. **249** (2009) 12. doi: https://doi.org/10.1016/j.desal.2009.06.008
11. *Malakootian, M., Mansoorian, H. J., Hosseini, A., Khanjani, N.*, Evaluating the efficacy of alumina/carbon nanotube hybrid adsorbents in removing Azo Reactive Red 198 and Blue 19 dyes from aqueous solutions, Process Saf. Environ. Prot. **96** (2015) 125. doi: https://doi.org/10.1016/j.psep.2015.05.002
12. *Dehghani, M., Shabestari, R., Anushiravani, A., Shamsedini, N.*, Application of electrocoagulation process for reactive red 198 dye removal from the aqueous solution, Iranian J. Health Sci. **2** (2014) 1.
13. *Jaafarzadeh, N., Omidinasab, M., Ghanbari, F.*, Combined electrocoagulation and UV-based sulfate radical oxidation processes for treatment of pulp and paper wastewater, Process Saf. Environ. Prot. **102** (2016) 462. doi: https://doi.org/10.1016/j.psep.2016.04.019
14. *Amin, M., Jaberian, B., Bina, B., Sadani, M., Hadian, R., Bonyadinejad, G., Moazzam, M. M. A.*, Advanced oxidation of the endosulfan and profenofos in aqueous solution using UV/H_2O_2 process, Environment Asia **7** (2014).
15. *Amin, M. M. Moazzam, M. M. A.*, Advanced oxidation treatment of composting leachate of municipal solid waste by ozone-hydrogen peroxide, Int. J. Environ. Health Eng. **3** (2014) 21.
16. *Amin, M. M. Moazzam, M. M. A.*, Use of a UV/H_2O_2 process for posttreatment of a biologically treated composting leachate, Turkish J. Eng. Env. Sci. **38** (2016) 404. doi: https://doi.org/10.3906/muh-1409-9
17. *Osugi, M. E., Rajeshwar, K., Ferraz, E. R., de Oliveira, D. P., Araújo, Â. R., Zanoni, M. V. B.*, Comparison of oxidation efficiency of disperse dyes by chemical and photoelectrocatalytic chlorination and removal of mutagenic activity, Electrochim. Acta. **54** (2009) 2086. doi: https://doi.org/10.1016/j.electacta.2008.07.015
18. *Gupta, V.*, Application of low-cost adsorbents for dye removal–A review, J. Environ. Manage. **90** (2009) 2313. doi: https://doi.org/10.1016/j.jenvman.2008.11.017
19. *Liu, P., Zhang, L.*, Adsorption of dyes from aqueous solutions or suspensions with clay nano-adsorbents, Sep. Purif. Technol. **58** (2007) 32. doi: https://doi.org/10.1016/j.seppur.2007.07.007
20. *Gupta, V. K., Kumar, R., Nayak, A., Saleh, T. A., Barakat, M.*, Adsorptive removal of dyes from aqueous solution onto carbon nanotubes: A review, Adv. Colloid Interface Sci. **193** (2013) 24. doi: https://doi.org/10.1016/j.cis.2013.03.003
21. *Xu, P., Zeng, G. M., Huang, D. L., Feng, C. L., Hu, S., Zhao, M. H., Lai, C., Wei, Z., Huang, C., Xie, G. X.*, Use of iron oxide nanomaterials in wastewater treatment: A review, Sci. Total Environ. **424** (2012) 1. doi: https://doi.org/10.1016/j.scitotenv.2012.02.023
22. *Zhu, H., Jiang, R., Li, J., Fu, Y., Jiang, S., Yao, J.*, Magnetically recyclable Fe_3O_4/Bi_2S_3 microspheres for effective removal of Congo red dye by simultaneous adsorption and photocatalytic regeneration, Sep. Purif. Technol. **179** (2017) 184. doi: https://doi.org/10.1016/j.seppur.2016.12.051
23. *Jaafarzadeh, N., Ghanbari, F., Ahmadi, M.*, Catalytic degradation of 2, 4-dichlorophenoxyacetic acid (2, 4-D) by nano-Fe_2O_3 activated peroxymonosulfate: Influential factors and mechanism determination, Chemosphere **169** (2017) 568. doi: https://doi.org/10.1016/j.chemosphere.2016.11.038
24. *Lu, A. H., Salabas, E. E. L., Schüth, F.*, Magnetic nanoparticles: synthesis, protection, functionalization, and application, Angew. Chem. Int. Ed. **46** (2007) 1222. doi: https://doi.org/10.1002/anie.200602866
25. *Manbohi, A. Ahmadi, S. H.*, In-tube magnetic solid phase microextraction of some fluoroquinolones based on the use of sodium dodecyl sulfate coated Fe_3O_4 nanoparticles packed tube, Anal. Chim. Acta. **885** (2015) 114. doi: https://doi.org/10.1016/j.aca.2015.05.030
26. *Jaafarzadeh, N., Amiri, H., Ahmadi, M.*, Factorial experimental design application in modification of volcanic ash as a natural adsorbent with Fenton process for arsenic removal, Environ. Technol. **33** (2012) 159. doi: https://doi.org/10.1080/09593330.2011.554887
27. *Atacan, K., Çakıroğlu, B., Özacar, M.*, Efficient protein digestion using immobilized trypsin onto tannin modified Fe_3O_4 magnetic nanoparticles, Colloids Surf B Biointerfaces. **156** (2017) 9. doi: https://doi.org/10.1016/j.colsurfb.2017.04.055
28. *Bagheri, H., Zandi, O., Aghakhani, A.*, Extraction of fluoxetine from aquatic and urine samples using sodium dodecyl sulfate-coated iron oxide magnetic nanoparticles followed by spectrofluorimetric determination, Anal. Chim. Acta. **692** (2011) 80. doi: https://doi.org/10.1016/j.aca.2011.02.060
29. *Faraji, M., Yamini, Y., Rezaee, M.*, Extraction of trace amounts of mercury with sodium dodecyle sulphate-coated magnetite nanoparticles and its determination by flow injection inductively coupled plasma-optical emission spectrometry, Talanta. **81** (2010) 831. doi: https://doi.org/10.1016/j.talanta.2010.01.023
30. *Shariati, S., Faraji, M., Yamini, Y., Rajabi, A. A.*, Fe_3O_4 magnetic nanoparticles modified with sodium dodecyl sulfate for removal of safranin O dye from aqueous solutions, Desalination. **270** (2011) 160. doi: https://doi.org/10.1016/j.desal.2010.11.040
31. *Zhao, X., Shi, Y., Wang, T., Cai, Y., Jiang, G.*, Preparation of silica-magnetite nanoparticle mixed hemimicelle sorbents for extraction of several typical phenolic compounds from environmental water samples, J. Chromatogr. A. **1188** (2008) 140. doi: https://doi.org/10.1016/j.chroma.2008.02.069
32. *Bhatti, H. N., Jabeen, A., Iqbal, M., Noreen, S., Naseem, Z.*, Adsorptive behavior of rice bran-based composites for mal-

achite green dye: Isotherm, kinetic and thermodynamic studies, J. Mol. Liq. **237** (2017) 322.
doi: https://doi.org/10.1016/j.molliq.2017.04.033

33. *Abbasi, M.*, Synthesis and characterization of magnetic nanocomposite of chitosan/SiO_2/carbon nanotubes and its application for dyes removal, J. Clean Prod. (2017)
doi: https://doi.org/10.1016/j.jclepro.2017.01.046
34. *Mor, S., Ravindra, K., Bishnoi, N.*, Adsorption of chromium from aqueous solution by activated alumina and activated charcoal, Bioresour. Technol. **98** (2007) 954.
doi: https://doi.org/10.1016/j.biortech.2006.03.018
35. *Tahir, M. A., Bhatti, H. N., Iqbal, M.*, Solar red and brittle blue direct dyes adsorption onto *Eucalyptus angophoroides* bark: Equilibrium, kinetics and thermodynamic studies, J Environ. Chem. Eng. **4** (2016) 2431.
doi: https://doi.org/10.1016/j.jece.2016.04.020
36. *Rashid, A., Bhatti, H. N., Iqbal, M., Noreen, S.*, Fungal biomass composite with bentonite efficiency for nickel and zinc adsorption: A mechanistic study, Ecol. Eng. **91** (2016) 459.
doi: https://doi.org/10.1016/j.ecoleng.2016.03.014
37. *Bharali, D. Deka, R. C.*, Preferential adsorption of various anionic and cationic dyes from aqueous solution over ternary CuMgAl layered double hydroxide, Colloids Surf. A Physicochem. Eng. Asp. **525** (2017) 64.
doi: https://doi.org/10.1016/j.colsurfa.2017.04.060
38. *Amuda, O. S., Olayiwola, A. O., Alade, A. O., Farombi, A. G., Adebisi, S. A.*, Adsorption of methylene blue from aqueous solution using steam-activated carbon produced from *Lantana camara* stem, J. Envir. Protect. **5** (2014) 1352.
doi: https://doi.org/10.4236/jep.2014.513129
39. *Adhikari, S., Mandal, S., Sarkar, D., Kim, D.-H., Madras, G.*, Kinetics and mechanism of dye adsorption on WO_3 nanoparticles, Appl. Surf. Sci. **420** (2017) 472.
doi: https://doi.org/10.1016/j.apsusc.2017.05.191
40. *Rajoriya, R., Prasad, B., Mishra, I., Wasewar, K.*, Adsorption of benzaldehyde on granular activated carbon: kinetics, equilibrium, and thermodynamic, Chem. Biochem. Eng. Q. **21** (2007) 219.
41. *Ho, Y.-S., McKay, G.*, Pseudo-second order model for sorption processes, Process Biochem. **34** (1999) 451.
doi: https://doi.org/10.1016/S0032-9592(98)00112-5
42. *Langmuir, I.*, The adsorption of gases on plane surfaces of glass, mica and platinum, J. Am. Chem. Soc. **40** (1918) 1361.
doi: https://doi.org/10.1021/ja02242a004
43. *Yang, C.-h.*, Statistical mechanical study on the Freundlich isotherm equation, J. Colloid Interface Sci. **208** (1998) 379.
doi: https://doi.org/10.1006/jcis.1998.5843
44. *Dada, A., Olalekan, A., Olatunya, A., Dada, O.*, Langmuir, Freundlich, Temkin and Dubinin–Radushkevich isotherms studies of equilibrium sorption of Zn^{2+} unto phosphoric acid modified rice husk, IOSR J. Appl. Chem. **3** (2012) 38.
45. *Radjenovic, A. Malina, J.*, Adsorption of organic acids on blast furnace sludge, Chem. Biochem. Eng. Q. **23** (2009) 187.
46. *Li, Y., Liu, T., Du, Q., Sun, J., Xia, Y., Wang, Z., Zhang, W., Wang, K., Zhu, H., Wu, D.*, Adsorption of cationic red X-GRL from aqueous solutions by graphene: Equilibrium, kinetics and thermodynamics study, Chem. Biochem. Eng. Q. **25** (2012) 483.